Phys. Med. Biol. **54** (2009) 3173–3183 doi:10.1088/0031-9155/54/10/014

The influence of a novel transmission detector on 6 MV x-ray beam characteristics

Sankar Venkataraman[1,2], Kyle E Malkoske[1], Martin Jensen[1], Keith D Nakonechny[1], Ganiyu Asuni[2] and Boyd M C McCurdy[1,2]

[1] Department of Medical Physics, CancerCare Manitoba, 675 McDermot Ave., Winnipeg, Manitoba, Canada
[2] Department of Physics and Astronomy, University of Manitoba, Winnipeg, Manitoba, Canada

E-mail: sankar.venkataraman@cancercare.mb.ca

Received 9 February 2009, in final form 1 April 2009
Published 6 May 2009
Online at stacks.iop.org/PMB/54/3173

Abstract

The purpose of this work was to investigate the influence of a new transmission detector on 6 MV x-ray beam properties. The device, COMPASS (IBA Dosimetry, Germany), contains 1600 plane parallel ionization chambers with a detector spacing of 6.5 mm and an active volume of 0.02 cm^3. Surface dose measurements were carried out using a Markus chamber and radiochromic film for a range of field sizes and source-to-surface distances (SSDs). The surface dose and dose in the build-up region for COMPASS fields were compared to open fields. For moderately narrow beam geometric conditions, the increase in surface dose was small. For the largest field size investigated (20×20 cm^2) at a 90 cm SSD, the surface dose with the detector was 34.9% versus 26.8% in the open field. However, the increase in surface dose in COMPASS fields was less than that observed with a standard block tray in the field (38.7% in the above example). It was found that beyond d_{max}, the difference in relative dose (profiles and PDDs) between open and COMPASS fields was insignificant. The mean transmission factor of the detector was 0.967 (standard deviation = 0.002) measured over a range of field sizes from 3×3 to 20×20 cm^2 at SSDs from 70 cm to 90 cm. In summary, the transmission detector was found to increase the relative dose in the buildup region but had a negligible effect on the beam parameters beyond d_{max}.

1. Introduction

Two-dimensional dosimeter arrays are used in modern radiotherapy to measure the complex dose distributions produced by dynamic fields, such as dynamic wedges or intensity-modulated radiation therapy (IMRT). These 2D arrays provide an efficient means of measuring the dose at multiple locations in the field. Several arrays are available that use ion chambers (Spezi *et al* 2005, Herzen *et al* 2007, Amerio *et al* 2004, Stasi *et al* 2005), diode detectors (Letourneau

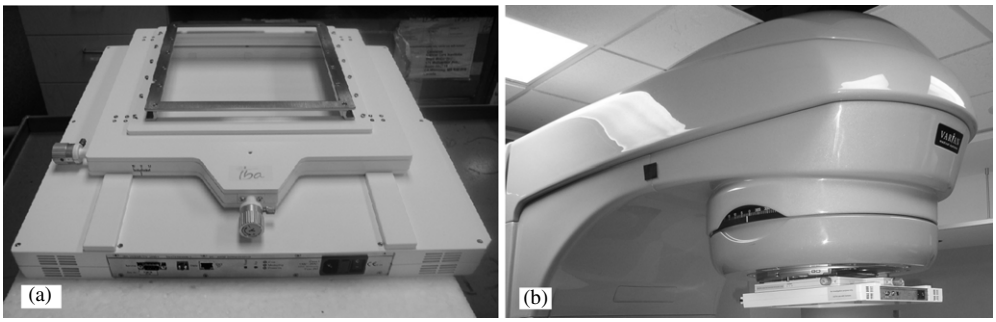

Figure 1. (a) COMPASS detector (b) COMPASS mounted on the gantry of a linear accelerator.

et al 2004, Jursinic and Nelms 2003), electronic portal imaging device (Greer *et al* 2007) or active matrix flat-panel dosimeter (El-Mohri *et al* 1999, Moran *et al* 2005). A new 2D ionization chamber array manufactured by IBA Dosimetry (Germany) is under evaluation at our center. The device is positioned in the upper wedge slot of the linear accelerator, providing the capability to perform real-time dose measurements during treatment delivery.

Since it is a new transmission device, its use for in-field measurements with a patient present necessitates a detailed study of its influence on the beam characteristics. Skin dose especially can be one of the limiting factors in treatment plans with high target doses and is a focus in this work, together with general transmission and patient dosimetry effects. Similar studies in the past have been completed for beam modifiers such as wedges, multi-leaf collimators (MLCs) and block trays (Kim *et al* 1998, McParland 1991, Lamb and Blake 1998, Butson *et al* 1998, Li and Klein 1997). In this paper, we present the transmission characteristics of this chamber array as well as its influence on the dose in the build-up region and beyond.

2. Methods and materials

2.1. Description of a COMPASS detector

COMPASS is a pixel-segmented ionization chamber. This dosimetry device is a 2D array of 1600 air-vented plane parallel chambers with an active area of 40 $\times$ 40 cm^2 projected at the isocenter and shown in figure 1. The external dimensions of this transmission device are 52 cm (W), 49 cm (L) and 11 cm (H) and weighs 15 kg. Each chamber is 3.8 mm in diameter and 2 mm in height. The chambers are spaced 6.5 mm apart, which projects to 1 cm at the isocenter. In our measurements, the detector assembly was mounted directly onto the gantry in the wedge slot of a Varian Clinac 2100iX linear accelerator with a source-to-detector distance of 65 cm.

All measurements were performed at 6 MV on a Varian 2100iX linear accelerator (linac) with Millennium 120-leaf MLC. The measurements covered a range of field sizes, source–surface distances (SSDs) and depths as necessary. In this work, 'COMPASS field' refers to a radiation field with the COMPASS detector in the beam path.

2.2. Measurement techniques

Extrapolation chambers have long been recognized as capable of accurate measurements of dose at the surface and in the build-up region of megavoltage x-ray beams (Yu *et al* 2003, Manson *et al* 1975). However, extrapolation chambers are not commonly available in therapy

centers due to their specialized application. Mellenberg (1990) compared the response of the Markus Model 329 parallel plate chamber (PTW-Freiburg, Germany) to that of an extrapolation chamber in the buildup region of megavoltage x-ray beams and generated tables of correction factors to account for the 'over-response' of the Markus chamber. The over-response is due to the small guard ring width in the Markus Model 329 design (Gerbi and Khan 1990). In this study, we used the Markus Model 329 chamber for measurements in the build-up region and corrected the raw measurement by a simple subtraction of the over-response factor based on Mellenberg's data.

To validate our Markus chamber measurements, we compared the doses at the surface and in the build-up region to those measured with GafChromic EBT film (International Specialty Products, Wayne, NJ) and calculated with Monte Carlo simulation. Recently, several authors have shown radiochromic film to also be a suitable dosimeter for dose measurements in the buildup region (Devic *et al* 2006, Quach *et al* 2000). The film measurements were performed in solid water slabs for a 10 × 10 cm^2 field size and a source-to-surface distance (SSD) of 90 cm with the film positioned perpendicular to the beam direction. The films were scanned in a Vidar Dosimetry Advantage Pro^{TM} digitizer (Vidar Systems Corporation, Herndon, VA). Film analysis was performed with RIT 113 software (Radiological Imaging Technology, Colorado Springs, CO) using a calibration curve based on 24 exposures ranging from 11 to 613 cGy to convert the optical density to dose (Childress *et al* 2002). Evaluation of the surface dose requires the extrapolation of film measurements since the effective measurement point is located at mid-thickness of the film, resulting in a minimum measurement depth of about 153 μm for EBT films.

For the Monte Carlo simulation, the treatment head of the linear accelerator was modeled using BEAMnrc/EGSnrc software (Rogers *et al* 1995) based on the specifications provided by the manufacturer. The beam model was validated by comparison of Monte Carlo simulation to measurements using a water phantom at 90 cm SSD and 20 × 20 cm^{-2} field size. The percentage depth doses and profiles at d_{max}, 5 cm, 10 cm and 20 cm were compared and the differences were within 2%. Phase-space files were generated for field sizes of 20 × 20 cm^2. The generated phase-space files contain position, energy, charge and weight of scored particles and were used as input in the DOSXYZnrc/EGSnrc for calculating dose in a water phantom. Electron kinetc energy transport cut-off and photon transport cut-off energy used for the beam simulation and dose calculations are 0.700 MeV and 0.010 MeV, respectively. An exact boundary crossing algorithm was run for accurate electron transport and the PRESTA-II electron step algorithm was used. The photon forcing and Rayleigh scattering options were turned off, but Russian roulette and uniform bremsstrahlung splitting, a variance reduction technique producing 40 bremsstrahlung photons for each bremsstrahlung event, were turned on to increase the efficiency of treatment head simulation. All the Monte Carlo simulations were performed with a maximum uncertainty of ±0.3% by increasing the number of particles.

To check the reproducibility of the Markus chamber and GafChromic film, the surface dose was independently measured five times under the same geometric conditions. The measurement uncertainty associated with the chamber and film were ±0.4% and ±0.7% (1 s.d.), respectively. The short-term reproducibility check with a reference chamber was performed to ascertain the linac output uncertainty and was found to be ±0.05%.

2.3. The influence of the transmission detector on the surface dose and in the build-up region

Surface doses, S, are reported as a percentage of the dose at a depth of 1.4 cm, which corresponds to the average depth of maximum dose (d_{max}) in an open field for the range of field sizes and SSDs studied. The surface dose on the central axis was measured for field sizes ranging from 3 × 3 to 20 × 20 cm^2 and SSDs from 70 to 90 cm for open and COMPASS fields.

Central axis percentage depth doses (PDDs) from the surface to a depth of 1.6 cm were measured using the Markus chamber in solid water, at a resolution of 2 mm. Measurements were performed in both open and COMPASS fields to evaluate how the presence of the detector affected the dose at shallow depths. A range of SSDs (70–90 cm) and field sizes (3×3 cm^2 to 20×20 cm^2) were evaluated.

To evaluate the influence of the transmission detector on the surface dose across the field, off-axis measurements (profiles) were performed using the Markus chamber in solid water for open and COMPASS fields. The chamber was positioned with the effective point of measurement at the surface and the profiles were acquired for a 20×20 cm^2 field at SSDs of 70, 80 and 90 cm. The profiles were measured to a distance of 20 cm from the central axis for all SSDs, at a resolution of 2–20 mm depending on the dose gradient.

It has been shown from previous studies that IMRT itself does not contribute to increased surface doses (Dogan and Glasgow 2003, Price *et al* 2006). In addition, the authors have observed that the increased surface dose due to beam obliquity in IMRT was similar to the increase in the dose with the use of open beams. Therefore, our detailed evaluations in this paper have been limited to open fields. However, a picket fence pattern representing the IMRT plan was irradiated with and without the COMPASS detector in field and the analysis was performed. The results showed that the increase in surface dose for picket fence with COMPASS compared to open field was similar to the increase observed for normal jaw settings. In other words, the COMPASS detector itself does not contribute to any increase in surface dose for IMRT plans.

2.4. The influence of the transmission detector on dose beyond d_{max}

Since the transmission detector is intended to be positioned in the beam during patient treatments, it is important to assess how the device influences the dose beyond $d_{\max}$ so that modifications to the treatment planning data may be incorporated if necessary (i.e. possibly adjusting the beam model). The following relative dose parameters were compared with and without the transmission detector in the path of the beam: central axis PDD; profiles at 1.4 and 10 cm depths; transmission factor at 10 cm. PDDs and profiles were measured in a water phantom using a Markus chamber and diode (PFD Scanditronix), respectively, for field sizes ranging from 3×3 cm^2 to 20×20 cm^2 and SSDs of 80 and 90 cm (the geometry of the water phantom did not allow measurements at a 70 cm SSD in COMPASS fields). The transmission factors were measured in solid water at 10 cm depth using a Markus chamber for field sizes ranging from 3×3 to 20×20 cm^2 and SSDs from 70 to 90 cm.

2.5. Comparison of the transmission detector to a block tray

A comparison of the transmission detector to a standard acrylic block tray was made to assess its influence on the beam relative to a common treatment accessory. A subset of the above measurements was repeated at a single SSD of 90 cm with the 5.8 mm thick acrylic Varian block tray in the accessory mount. These measurements included PDDs from the surface to a depth of 20 cm, and transmission factor measurements.

3. Results

3.1. The influence of the transmission detector on the surface dose and dose within the buildup region

There was good agreement between the doses measured with the Markus chamber, EBT film and Monte Carlo simulation in the build-up region (figure 2). The surface doses, S (90 cm,

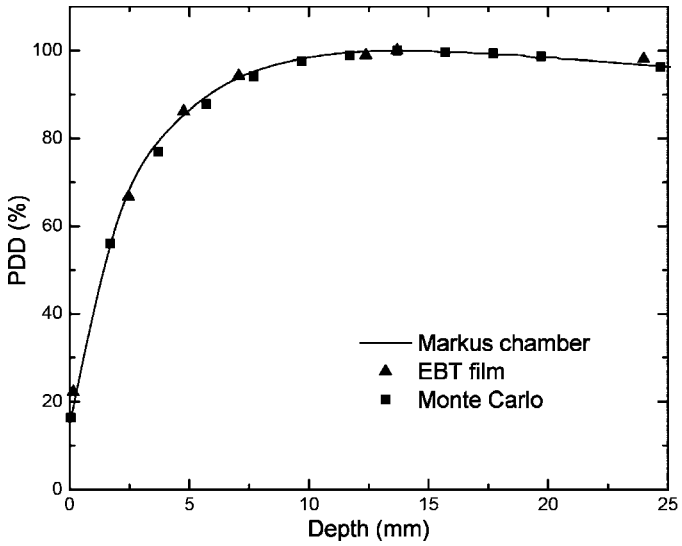

Figure 2. Comparison of the dose in the buildup region measured in solid water with a Markus chamber and EBT film, and the calculated dose from Monte Carlo simulation for an open field of 10×10 cm^2 and an SSD of 90 cm.

Table 1. The difference between the surface doses in open and COMPASS fields. Differences are expressed as a percentage of the dose at 1.4 cm depth, i.e. S (COMPASS field) $-$ S (open field). The measured surface doses in the open fields (percentage of the dose at 1.4 cm depth) are shown in parentheses for reference.

	S(COMPASS) $-$ S(open) (%)		
Field size (cm^2)	SSD = 90 cm	SSD = 80 cm	SSD = 70 cm
3×3	0.7 (6.4)	1.4 (6.5)	8.7 (7.1)
5×5	1.3 (8.6)	3.0 (8.7)	18.2 (9.7)
10×10	3.0 (14.8)	8.1 (15.3)	36.3 (17.4)
20×20	8.1 (26.8)	18.2 (28.5)	44.8 (32.6)

10×10 cm^2), were 14.8% and 14.6% for the Markus chamber and EBT film, respectively, while the Monte Carlo calculated surface dose (at 50 μm) was 16.3%.

The surface dose and dose in the buildup region increased when the transmission detector was in the beam as shown in figure 3 and table 1. The error bars for all the measurements are within the size of data points and hence not explicitly shown. For moderately narrow beam geometric conditions (smaller fields, larger SSDs), the increase in surface dose was small. However, as the field size increased or in particular, the SSD was reduced, the increase in surface dose became quite large. For example, at an SSD of 70 cm the surface dose with the transmission detector in the beam was more than double that of the open field. For the 20×20 cm^2 field at a 70 cm SSD, the depth of $d_{\max}$ was shifted from 14 mm to 5 mm when the transmission detector was in the beam.

In broader terms, the surface dose profiles showed expected behavior within the field, i.e. increased doses for COMPASS compared to open fields. Results of surface dose profiles for SSDs 70 cm and 90 cm are presented in figure 4. Open-field central axis dose was used for

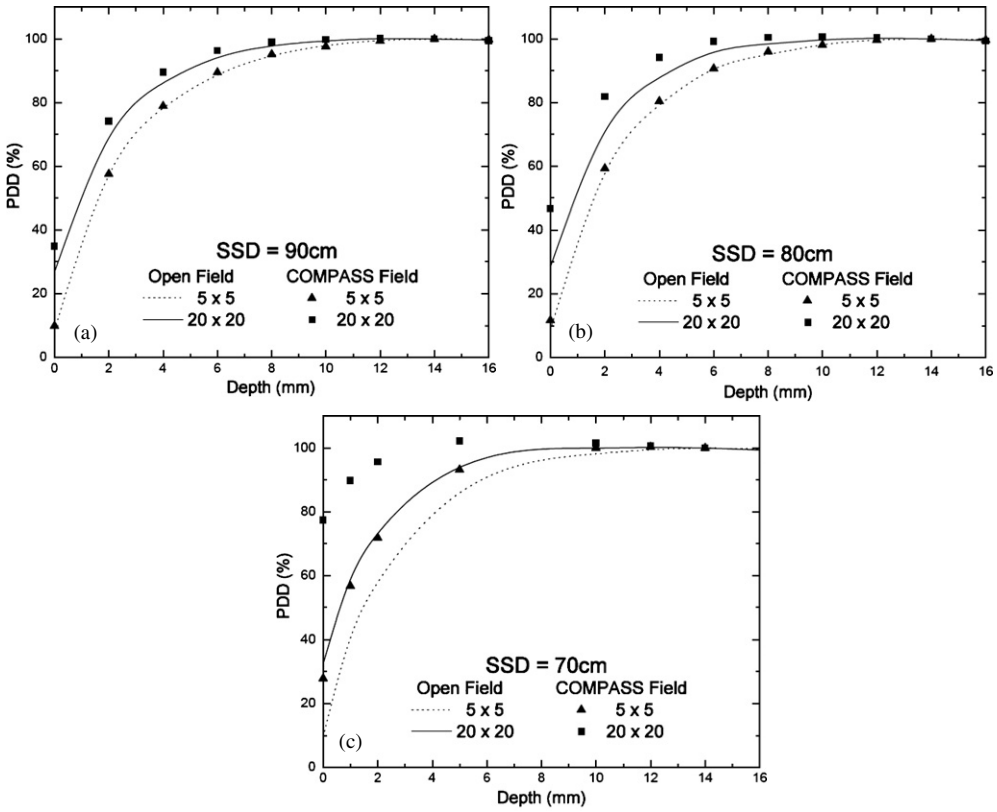

Figure 3. The dose in the buildup region at SSDs of (a) 90 cm, (b) 80 cm and (c) 70 cm. The lines indicate measured doses in the open field, whereas the symbols represent doses measured with the transmission detector in the beam. All the measurements were performed with the Markus chamber in solid water.

normalization for both open and COMPASS fields. Off-axis doses for the COMPASS field were much larger and less uniform than the open field for an SSD of 70 cm. As the SSD increased from 70 cm to 90 cm, the dose differences decreased and the COMPASS profiles showed more uniformity. Figure 4(c) illustrates the surface dose difference as a percentage of the open field central axis dose for all three SSDs. It was interesting to note that COMPASS doses beyond the field edge for an SSD of 70 cm were lower than that of the open field while they were consistently higher than that of open fields for SSDs 80 cm and 90 cm. For example, at 6 cm beyond the field edge, the COMPASS dose for an SSD of 70 cm was 3% lower than that of the open field whereas it was 7.3% higher than that of the open field for both SSDs 80 cm and 90 cm, respectively.

3.2. The influence of the transmission detector on dose beyond d_{max}

Beyond $d_{\max}$, the differences between the PDDs and profiles were negligible, as shown in figures 5 and 6. The maximum difference between open and COMPASS fields was less than 0.3% of dose at $d_{\max}$.

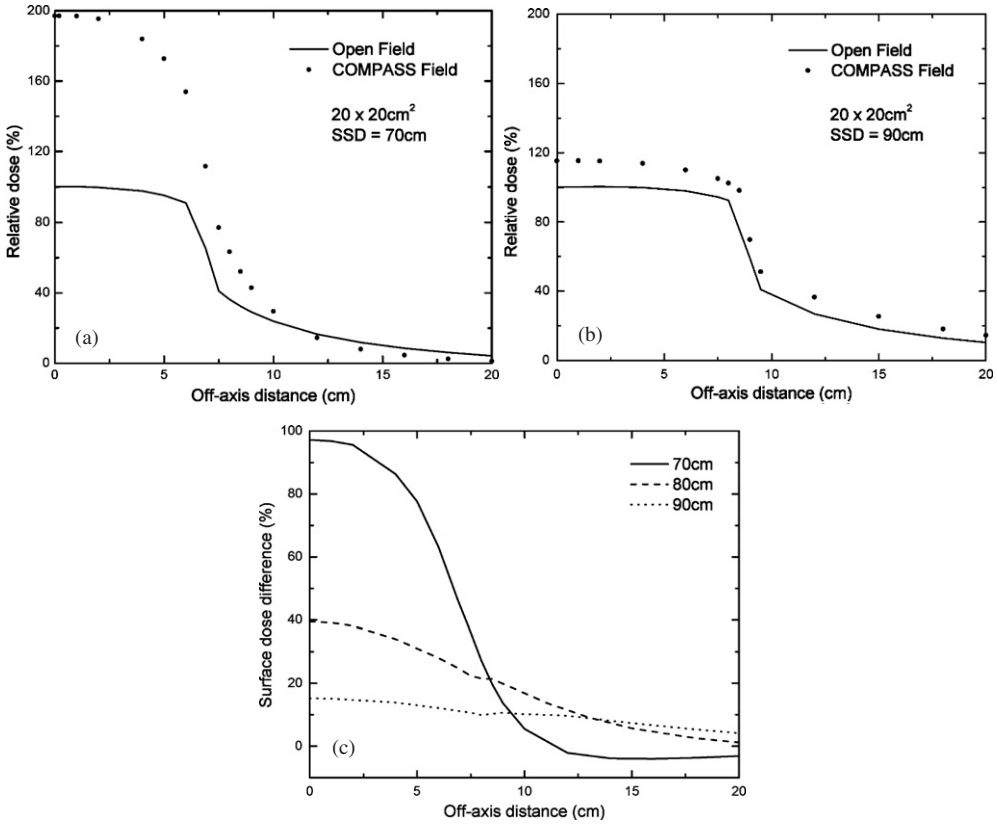

Figure 4. The surface dose profile at SSDs of (a) 70 cm and (b) 90 cm for 20 × 20 cm^2 field size. The lines indicate measured doses in the open field, whereas the symbols represent doses measured with the transmission detector in the beam. Measurements were taken with the Markus chamber in solid water; (c) shows the difference between the surface dose profile with and without the transmission detector in the beam expressed as a percentage of the open field dose on the central axis. Data for the three SSDs show the reduction in surface dose in-field and increase in surface dose out-of-field as the SSD increases, due to the lateral divergence of the electrons produced in the transmission detector.

The transmission factors were very consistent throughout the range of field sizes, off-axis distances and SSDs investigated (the same range as in table 1). The mean value was 0.967 with a standard deviation of 0.002.

3.3. Comparison of the transmission detector to a block tray

When comparing the transmission detector to a standard acrylic block tray, it was found that the two accessories had a similar effect on the beam properties, as shown in table 2. The transmission factor for the COMPASS detector was found to be 0.4% lower than that for the block tray. The surface doses with the transmission detector were consistently lower than those with the block tray. The maximum difference in surface dose was at the 20 × 20 cm^2 field, where the transmission detector had a surface dose 3.8% lower than that of the block tray. Figure 7 demonstrates the similarity in PDD between the two accessories.

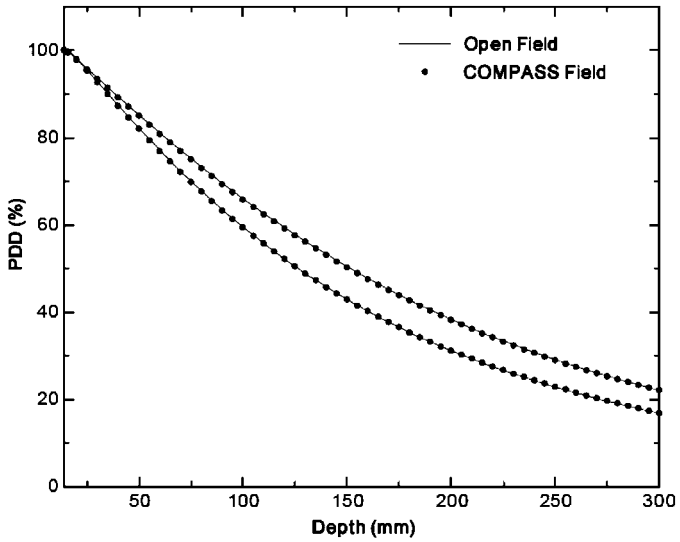

Figure 5. PDDs beyond d_{max} for 5 × 5 cm^2 (lower curve) and 20 × 20 cm^2 fields at an SSD of 80 cm. The first measurement point is at d_{max} in the figure. Measurements were taken with the Markus chamber in the water phantom. Similar results were obtained at 70 cm and 90 cm SSDs.

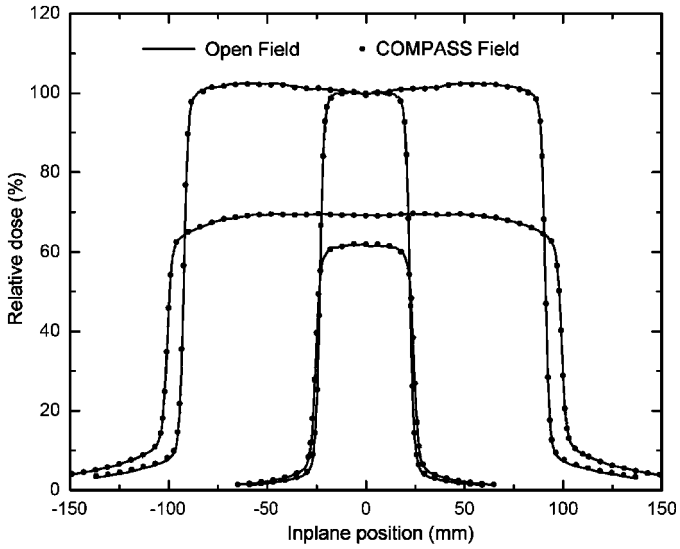

Figure 6. Profiles at 1.4 cm and 10 cm depths for 5 × 5 cm^2 and 20 × 20 cm^2 fields at an SSD of 90 cm. Measurements were taken with the diode in the water phantom.

4. Discussion

The dose in the buildup region of a 6 MV beam was affected by the presence of the COMPASS transmission detector. Butson *et al* (1996) studied in detail the causes for the surface dose and dose in the build-up region and concluded that the surface dose at 6 MV is mostly due

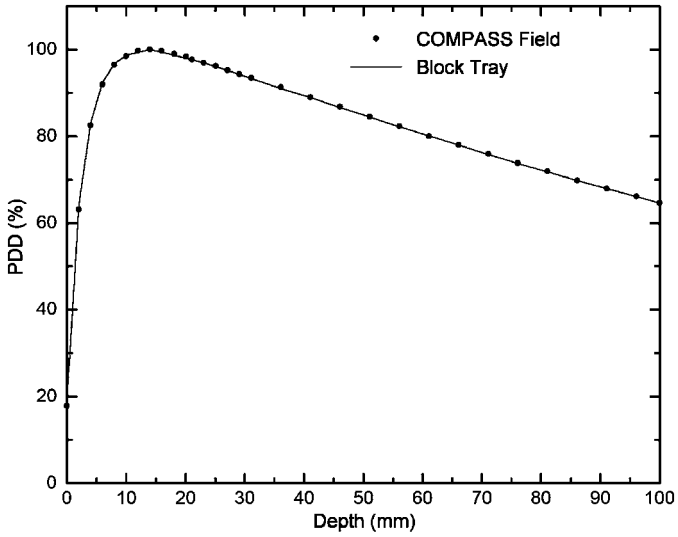

Figure 7. The percentage depth dose with the transmission detector or a block tray in the field. The data are obtained at an SSD of 90 cm using a 10 × 10 cm^2 field using the Markus chamber in the water phantom. Similar results were obtained for other field sizes with the only appreciable difference being noted at the surface of the water phantom.

Table 2. Comparison of the surface dose, *S*, and the transmission factor, *TF*, for the transmission detector and a standard Varian acrylic block tray. Note that the *TF* data are the average of the four field sizes at a 90 cm SSD.

Parameter	Transmission detector	Block tray
S (3 × 3 cm^2)	7.1%	7.6%
S (5 × 5 cm^2)	9.9%	10.7%
S (10 × 10 cm^2)	17.8%	19.6%
S (20 × 20 cm^2)	34.9%	38.7%
TF	0.967	0.971

to electron contamination. At a short distance between the transmission detector and the phantom surface (SSD 70 cm), the surface dose on the central axis measured in this study increased by approximately a factor of 2 for all field sizes as compared to that measured at a 90 cm SSD. As the SSD increased, the elevation of surface dose with the detector inserted was less pronounced. For the largest field size investigated at a 90 cm SSD, the surface dose with the detector inserted was 34.9% versus 26.8% in the open field. With the transmission detector serving as an extra source of electron contamination to the beam, this behavior was expected. In fact, the increases in surface dose with the detector in beam (table 1) exhibited roughly an inverse-square law dependence with respect to a position 65 cm from the x-ray target for the 3 × 3 and 5 × 5 cm^2 field sizes. This corresponded to approximately the center of the transmission detector. At a given SSD, the influence of the transmission detector on surface dose was more pronounced as the field size increased.

In general, the observed increase in surface dose with COMPASS can be attributed to increased electron contamination with the detector acting as an extended electron source. At

an SSD of 70 cm, there was less than 5 cm air gap between the exit surface of the transmission detector and the phantom surface. Due to the short distance between the site of electron liberation in the transmission detector and the surface of the phantom, there was little angular spread and hence the majority of the added contaminant electrons intercepted the phantom within the geometric boundary of the photon field. As the SSD increased, the change in surface doses with off-axis position diminished and became more evenly distributed between the in- and out-of-field regions at the phantom surface (figure 4(c)).

The increased surface dose at smaller SSDs should be kept in mind when treating obese patients with the COMPASS detector inserted as the surface dose at SSD = 70 cm increases from 32.6% for the open field to 77.4% for the COMPASS field. In these rare cases, the treatment may require a larger number of beams to spread out the excess surface dose or removal of the device from the beam during treatment.

The PDDs in the buildup region of open and COMPASS fields gradually merged with depth as the influence of photon phantom scatter started to dominate the electron contamination component of dose. The PDD and profiles beyond the average d_{max} depth of 14 mm were not significantly affected by the presence of the transmission detector. Based on our observations, no changes to the treatment planning system's open field model would be required for treatment delivery with COMPASS in the beam, other than a scaling of the monitor units by the detector transmission factor.

The transmission factor showed very little variation with field size and SSD (standard deviation <0.2%). It is suggested that a single value of transmission factor (in our case 0.967) be applied to all field geometries for the linac and energy studied here. When this information is factored into the treatment plans, the actual dose distribution can be obtained with the detector in the beam path. Comparison to measurements with an acrylic block tray has shown that the insertion of the transmission detector has a similar effect on the radiation beam as a standard block tray.

5. Conclusion

This work describes the influence of a new transmission detector consisting of a 2D ionization chamber array on 6 MV photon beam dosimetry. An increase in the surface dose was observed with the detector in the beam path for large field sizes and small SSDs. Due to the increased surface dose for shorter SSDs (e.g. 70 cm), it may be prudent to either remove the detector for obese patient treatments or to modify the treatment plan to redistribute the doses to minimize the local surface dose. Our measurements show that the differences between open and COMPASS fields were found to be insignificant beyond d_{max}. A single transmission factor of 0.967 could be entered in the beam data of the treatment planning system as this factor was nearly constant over a large range of SSDs and field sizes. The similarity in the effect of the block tray and transmission detector on the beam parameters is reassuring. With the exception of the transmission factor, the only influence of the transmission detector on a 6 MV beam is an increase in dose in the buildup region. Beyond d_{max}, the beam parameters of COMPASS and open fields were in good agreement.

Acknowledgments

The authors wish to thank L Mueller (IBA Dosimetry, Schwarzenbruck, Germany) for his help and discussion during the work. This work was supported in part by IBA Dosimetry.

References

Amerio S *et al* 2004 Dosimetric characterization of a large area pixel-segmented ionization chamber *Med. Phys.* **31** 414–20

Butson M J, Perez M D, Mathur J N and Metcalfe P E 1996 6 MV x-ray dose in the build up region: empirical model and the incident angle effect *Australas. Phys. Eng. Sci. Med.* **19** 74–82

Butson M J, Yu P K and Metcalfe P E 1998 Measurement of off-axis and peripheral skin dose using radiochromic film *Phys. Med. Biol.* **43** 2647–50

Childress N L, Dong L and Rosen I I 2002 Rapid radiographic film calibration for IMRT verification using automated MLC fields *Med. Phys.* **29** 2384–90

Devic S, Seuntjens J, Abdel-Rahman W, Evans M, Olivares M, Podgorsak E B, Te V and Christopher G S 2006 Accurate skin dose measurements using radiochromic film in clinical applications *Med. Phys.* **33** 1116–24

Dogan N and Glasgow G P 2003 Surface and build-up region dosimetry for obliquely incident intensity modulated radiotherapy 6 MV x rays *Med. Phys.* **30** 3091–6

El-Mohri Y, Antonuk L E, Yorkston J, Jee K W, Maolinbay M, Lam K L and Siewerdsen J H 1999 Relative dosimetry using active matrix flat-panel imager (AMFPI) technology *Med. Phys.* **26** 1530–41

Gerbi B J and Khan F M 1990 Measurement of dose in the buildup region using fixed-separation plane-parallel ionization chambers *Med. Phys.* **17** 17–26

Greer P B, Vial P, Oliver L and Baldock C 2007 Experimental investigation of the response of an amorphous silicon EPID to intensity modulated radiotherapy beams *Med. Phys.* **34** 4389–98

Herzen J, Todorovic M, Cremers F, Platz V, Albers D, Bartels A and Schmidt R 2007 Dosimetric evaluation of a 2D pixel ionization chamber for implementation in clinical routine *Phys. Med. Biol.* **52** 1197–208

Jursinic P A and Nelms B E 2003 A 2-D diode array and analysis software for verification of intensity modulated radiation therapy delivery *Med. Phys.* **30** 870–9

Kawrakow I and Rogers D W O 2003 The EG Snrc Code System: Monte Carlo simulation of electron and photon transport *Technical Report PIRS-701* National Research Council of Canada, Ottawa

Kim S, Liu C R, Zhu T C and Palta J R 1998 Photon beam skin dose analyses for different clinical setups *Med. Phys.* **25** 860–6

Lamb A and Blake S 1998 Investigation and modelling of the surface dose from linear accelerator produced 6 and 10 MV photon beams *Phys. Med. Biol.* **43** 1133–46

Letourneau D, Gulam M, Yan D, Oldham M and Wong J W 2004 Evaluation of a 2D diode array for IMRT quality assurance *Radiother. Oncol.* **70** 199–206

Li Z and Klein E E 1997 Surface and peripheral doses of dynamic and physical wedges *Int. J. Radiat. Oncol. Biol. Phys.* **37** 921–5

Manson D J, Velkley D, Purdy J A and Oliver G D J 1975 Measurements of surface dose using build-up curves obtained with an extrapolation chamber *Radiology* **115** 473–4

McParland B J 1991 The effects of a universal wedge and beam obliquity upon the central axis dose buildup for 6-MV x-rays *Med. Phys.* **18** 740–3

Mellenberg D E Jr 1990 Determination of build-up region over-response corrections for a Markus-type chamber *Med. Phys.* **17** 1041–4

Moran J M, Roberts D A, Nurushev T S, Antonuk L E, El-Mohri Y and Fraass B A 2005 An active matrix flat panel dosimeter (AMFPD) for in-phantom dosimetric measurements *Med. Phys.* **32** 466–72

Nathan L C, Lei D and Isaac I R 2002 Rapid radiographic film calibration for IMRT verification using automated MLC fields *Med. Phys.* **29** 2384–90

Price S, Williams M, Butson M and Metcalfe P 2006 Comparison of skin dose between conventional radiotherapy and IMRT *Australas. Phys. Eng. Sci. Med.* **29** 272–7

Quach K Y, Morales J, Butson M J, Rosenfeld A B and Metcalfe P E 2000 Measurement of radiotherapy x-ray skin dose on a chest wall phantom *Med. Phys.* **27** 1676–80

Rogers D W O, Faddegon B A, Ding G X, Ma C M, We J and Mackie T R 1995 BEAM: a Monte Carlo code to simulate radiotherapy treatment units *Med. Phys.* **22** 503–24

Spezi E, Angelini A L, Romani F and Ferri A 2005 Characterization of a 2D ion chamber array for the verification of radiotherapy treatments *Phys. Med. Biol.* **50** 3361–73

Stasi M *et al* 2005 D-IMRT verification with a 2D pixel ionization chamber: dosimetric and clinical results in head and neck cancer *Phys. Med. Biol.* **50** 4681–94

Yu P K, Cheung T and Butson M J 2003 Variations in skin dose using 6 MV or 18 MV x-ray beams *Australas. Phys. Eng. Sci. Med.* **26** 79–81